

CAPT: Class-Aware Prompt Tuning for Federated Long-Tailed Learning with Vision-Language Model

Shihao Hou¹ Xinyi Shang² Shreyank N Gowda³ Yang Lu^{1*} Chao Wu⁴ Yan Yan¹ Hanzi Wang¹
¹Xiamen University ²University College London ³University of Nottingham ⁴Zhejiang University
 houshihao@stu.xmu.edu.cn, xinyi.shang.23@ucl.ac.uk, Shreyank.Narayanagowda@nottingham.ac.uk,
 luyang@xmu.edu.cn, chao.wu@zju.edu.cn, yanyan@xmu.edu.cn, hanzi.wang@xmu.edu.cn

Abstract

Effectively handling the co-occurrence of non-IID data and long-tailed distributions remains a critical challenge in federated learning. While fine-tuning vision-language models (VLMs) like CLIP has shown to be promising in addressing non-IID data challenges, this approach leads to severe degradation of tail classes in federated long-tailed scenarios. Under the composite effects of strong non-IID data distribution and long-tailed class imbalances, VLM fine-tuning may even fail to yield any improvement. To address this issue, we propose Class-Aware Prompt Learning for Federated Long-tailed Learning (CAPT), a novel framework that leverages a pre-trained VLM to effectively handle both data heterogeneity and long-tailed distributions. CAPT introduces a dual-prompt mechanism that synergizes general and class-aware prompts, enabling the framework to capture global trends while preserving class-specific knowledge. To better aggregate and share knowledge across clients, we introduce a heterogeneity-aware client clustering strategy that groups clients based on their data distributions, enabling efficient collaboration and knowledge sharing. Extensive experiments on various long-tailed datasets with different levels of data heterogeneity demonstrate that CAPT significantly improves tail class performance without compromising overall accuracy, outperforming state-of-the-art methods in federated long-tailed learning scenarios.

1. Introduction

Federated learning (FL) [22] enables multiple parties to collaboratively train a shared model without exposing private data, providing a privacy-preserving solution for leveraging distributed data to build powerful machine learning models [37]. However, FL faces substantial challenges in real-world scenarios, primarily due to the coexistence of non-independent and identically distributed (non-IID) data

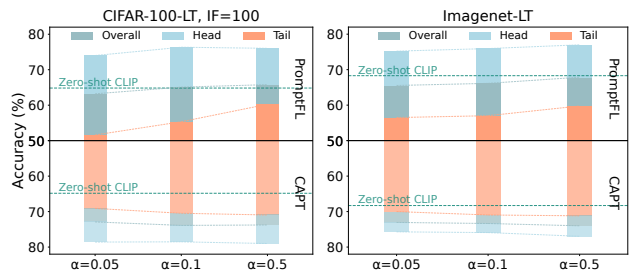


Figure 1. Performance comparison between PromptFL (upper part) and our proposed CAPT (lower part) on CIFAR-100-LT and ImageNet-LT. As client heterogeneity increases (α decreases from 0.5 to 0.05), PromptFL exhibits an expanding performance gap between head and tail classes, with overall accuracy even falling below zero-shot CLIP baseline (dashed line). In contrast, CAPT effectively mitigates the impact of client heterogeneity and significantly reduces the head-tail performance disparity while maintaining superior overall accuracy across all settings.

and long-tailed distributions. In federated settings, local data distributions vary significantly across clients [11, 46], and real-world data often follows a long-tailed distribution, where a few classes (head classes) have abundant samples, while the majority (tail classes) are severely underrepresented [20, 45]. The combination of non-IID data distribution and long-tailed class imbalance exacerbates the bias towards head classes. This issue is particularly challenging for tail classes, as their scarce samples are further fragmented across heterogeneous clients. Such fragmentation significantly complicates the learning of effective representations for these underrepresented classes [15, 16].

This composite problem, known as federated long-tailed learning, has attracted increasing attention in recent years [9, 29, 35, 36, 43]. To address these challenges, researchers have proposed various approaches [3, 17, 21, 39, 41]. These methods can be broadly categorized into data-centric and model-centric strategies. Data-centric methods aim to alleviate class imbalance by generating synthetic features for tail classes or aggregating features from both local and global models. Model-centric methods focus on adapting

*Corresponding Author: Yang Lu (luyang@xmu.edu.cn)

the learning process. However, these methods may introduce noise that disrupts model robustness and risk overfitting on minority classes, leading to inconsistency between local and global models [15]. Moreover, most existing methods have been designed for traditional FL settings and may not fully exploit the potential of emerging techniques, such as prompt learning with pre-trained models [12, 48].

Recently, the success of pre-trained vision-language models, such as CLIP [24], has opened up new possibilities for FL. These foundation models, trained on massive image-text pairs, have demonstrated remarkable generalization capabilities and transferability to various downstream tasks [44]. By adapting pre-trained models to specific tasks using lightweight prompt tuning, researchers have developed federated prompt learning [6], where prompts are learned locally at clients and periodically aggregated at the server to share knowledge across the federation. This approach has shown promise in addressing the non-IID problem while reducing communication overhead [19].

However, despite these advances, the effectiveness of CLIP and prompt-tuning methods in federated learning under long-tailed distributions remains largely unexplored. It is unclear whether these approaches can successfully address the unique challenges posed by long-tailed data in federated settings. To investigate this, we conducted a preliminary investigation into the application of prompt tuning techniques in federated long-tailed scenarios. Our findings, as illustrated in Fig. 1, reveal a significant challenge: *while prompt tuning improves overall performance in FL, it simultaneously exacerbates the long-tail problem*. As the degree of client heterogeneity increases, the performance gap between head and tail classes widens significantly. Notably, tail classes suffer from substantial performance degradation, leading to a decline in model accuracy under high heterogeneity conditions. This unexpected phenomenon highlights the limitations of current prompt-tuning approaches in federated long-tailed learning and raises three key research questions:

RQ 1: What causes prompt tuning to disproportionately affect tail classes in federated long-tailed scenarios?

RQ 2: How can we leverage the power of pre-trained vision-language models while addressing the problem of the sharp decrease in performance for the tail categories brought about by non-IID data?

RQ 3: Is there a way to improve tail class performance without sacrificing head class accuracy?

To answer the above-mentioned key questions, we propose Class-Aware Prompt Tuning (CAPT) for federated long-tailed learning, leveraging a pre-trained vision-language model. The core of our approach is a dual-prompt learning mechanism, which introduces a general prompt to learn domain-invariant features and class-aware prompts to capture fine-grained information for each class, particularly

benefiting tail classes. To facilitate prompt aggregation in an FL setting, we propose a heterogeneity-aware client clustering strategy that groups clients based on their data distributions, enabling efficient knowledge sharing among clients with similar long-tailed characteristics.

Our extensive empirical study demonstrates that CAPT effectively bridges the performance gap between head and tail classes while unveiling the potential of prompt tuning in federated long-tailed scenarios. Furthermore, we provide a theoretical analysis that formally characterizes why traditional prompt tuning methods struggle with federated long-tailed learning. The main contributions of this work are:

- We reveal the limitations of existing prompt tuning-based methods in FL under long-tailed data distributions, highlighting their negative impact on tail class performance and the need for novel solutions addressing the joint problem of non-IID and long-tailed data.
- We propose CAPT, a novel framework introducing class-aware prompts and heterogeneity-aware client clustering, which effectively addresses the challenges of federated long-tailed learning using pre-trained VLM.
- Our approach achieves state-of-the-art performance on multiple long-tailed datasets, significantly improving tail class performance while maintaining competitive overall accuracy in federated learning scenarios.

2. Related works

2.1. Federated Long-Tailed Learning

Federated learning with long-tailed data distribution has emerged as a critical research topic, addressing the challenges posed by data heterogeneity and class imbalance across clients. Early attempts focused on adapting loss functions to handle class imbalance in the federated setting. Fed-Focal Loss [27] and Ratio Loss [33] introduced re-weighting strategies in local training. However, these approaches often struggled with representation learning and relied on impractical assumptions about global class distributions. To address these limitations, subsequent works shifted towards feature-based solutions. FEDIC [28] pioneered the use of decoupled training, separating feature learning and classifier adaptation. Building upon this idea, CReFF [29] further improved performance through auxiliary datasets and refined classifier re-training, though its effectiveness was constrained by federated feature quality.

More recent works have focused on enhancing the quality of feature representation and classifier learning by incorporating additional information and techniques. Zeng et al. [43] proposed a global balanced multi-expert framework, which used a global proxy estimated from uploaded client gradients to guide client grouping and train a multi-expert model. Fed-GraB [36] and RedGrape [38] utilized global statistics to guide local training, with Fed-GraB in-

roducing adaptive gradient balancing and RedGrape incorporating gradient prototypes. CLIP2FL [30] leveraged the vision-language model CLIP to guide both client and server model training, and FedLoGe [35] enhanced performance through representation learning and classifier alignment within a neural collapse framework. It uses a sparsified classifier to enhance representation learning by pruning noisy features and realigns the backbone to the server and clients based on classifier weight norms.

While these methods have shown promising results, they often struggle to effectively balance the trade-off between maintaining global model consistency and addressing local data imbalances. Additionally, many of these approaches require significant computational resources or rely on assumptions about client data availability that may not hold in real-world federated scenarios [15].

2.2. Prompt Learning in Vision-Language Models

Prompt learning has emerged as a promising approach for adapting large-scale VLMs [24] to downstream tasks while preserving their generalization capabilities. CoOp [48] and CoCoOp [47] learned text prompts to adapt CLIP’s language branch, with CoCoOp enhancing generalization to novel classes through image-conditioned prompts. MaPLe [12] extended prompt learning to both vision and language branches, demonstrating the benefits of a complete prompting approach. Other works have explored various aspects of prompt learning, such as text-to-text optimization [1, 40], multi-label recognition [31], and unsupervised adaptation [8]. These approaches have shown significant improvements in adapting pre-trained VLMs to specific tasks.

Recent research has extended prompt learning to federated learning environments. PromptFL [6] initiated this direction by replacing traditional model training with prompt learning in distributed settings. FedOTP [14] and FedPGP [4] further explored prompt-based knowledge sharing and personalization strategies in federated settings. However, these methods primarily focus on addressing data heterogeneity and do not explicitly tackle the challenges posed by long-tailed data distributions in federated settings. Consequently, they often struggle with inconsistent client updates due to class imbalance and missing classes, leading to decreased performance in tail classes, particularly in scenarios with high client heterogeneity.

In contrast to these approaches, our proposed CAPT framework directly tackles the challenges of federated learning with long-tailed data distributions. By introducing class-aware prompts and a heterogeneity-aware client clustering strategy, CAPT enables more effective learning from imbalanced data across clients while maintaining communication efficiency. This novel approach not only addresses the class imbalance issue but also mitigates the negative effects of client heterogeneity on tail class performance.

3. Proposed Method

In this section, we present CAPT, a framework tailored for federated learning with long-tailed data. CAPT combines a dual-prompt mechanism—consisting of a general prompt for shared features and class-aware prompts for class-specific knowledge—with a heterogeneity-aware client clustering strategy. This clustering strategy consists of two complementary components: similarity-based clustering groups clients with similar data distributions to enhance tail class learning, and heterogeneity-based clustering balances head and tail class representation across clusters. Additionally, a Multi-Armed Bandit (MAB) scheduler optimizes communication efficiency by dynamically adjusting aggregation frequency. The entire framework is shown in Fig. 2.

3.1. Preliminaries

We consider a FL system with K clients and a central server, where each client k has a local dataset $D_k = \{(\mathbf{x}_i, y_i)\}_{i=1}^{|D_k|}$ with $\mathbf{x}_i \in \mathbb{R}^d$ and $y_i \in \{1, \dots, C\}$. The global dataset $D = \bigcup_{k=1}^K D_k$ follows a long-tailed distribution [32], with classes ordered as $n_1 \geq n_2 \geq \dots \geq n_C$, where n_c is the sample count for class c . We define classes with larger n_c as head classes and those with smaller n_c as tail classes. The non-IID data distribution across clients is simulated using a Dirichlet distribution with parameter α , creating varying imbalance patterns among clients.

Our work builds upon the CLIP model [24], which learns visual concepts from natural language supervision. CLIP consists of an image encoder $f(\mathbf{x})$ and a text encoder $g(\mathbf{t})$, both mapping inputs to a shared d -dimensional embedding space. The image encoder can be a convolutional neural network or a vision transformer (ViT), while the text encoder is typically transformer-based.

To adapt CLIP for downstream tasks without fine-tuning the entire model, we employ prompt learning [48]. This technique optimizes text prompts used to represent different classes. Hand-crafted prompts are replaced with learnable prompts as $\mathbf{t}_i = [\mathbf{V}_1, \mathbf{V}_2, \dots, \mathbf{V}_M, \text{CLASS}_i]$, where $[\mathbf{V}_1, \mathbf{V}_2, \dots, \mathbf{V}_M]$ are M learnable context tokens and CLASS_i is the name of class i . These context tokens can be randomly initialized or initialized with pre-trained word embeddings and then optimized to improve model performance.

3.2. Dual-Prompt Learning Mechanism

In federated long-tail scenarios, conventional prompt tuning methods face significant challenges when encountering long-tailed data distributions, where tail class samples are not only limited but also unevenly distributed across clients. To address these challenges, we propose a novel federated prompt learning mechanism with three complementary components: a *general prompt* that learns universal features shared across all classes to maintain model ro-

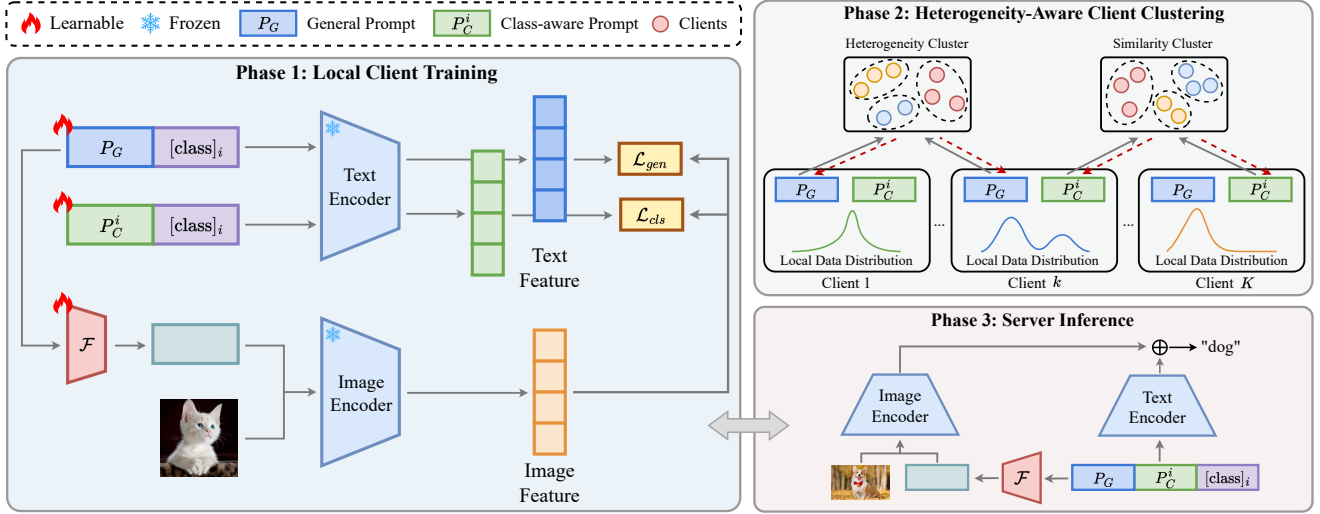


Figure 2. An overview of our proposed CAPT framework.

business, *class-aware prompts* that enables more nuanced feature representations for each specific class, and a *vision-language alignment* mechanism that bridges the semantic gap between visual and textual modalities. Our design particularly benefits tail classes through a synergistic combination: the general prompt provides robust common features learned from abundant data of all classes, while class-aware prompts capture fine-grained discriminative features specific to each class.

We also provide a theoretical analysis to formally characterize the challenges in federated long-tailed learning with prompt tuning methods. Our analysis reveals that the gradient variance in conventional methods increases proportionally with both the imbalance ratio and client heterogeneity, leading to slower convergence and degraded performance, particularly on tail classes. The complete Theorem 1 and Theorem 2 and their proofs can be found in Appendix F. This theoretical analysis answers RQ1 by revealing why prompt tuning methods struggle with tail classes in federated long-tailed scenarios.

General Prompt. We introduce a learnable general prompt \mathbf{P}_g to capture universal features shared by all classes. This general prompt serves as a foundation for learning domain-invariant representations, which is crucial for maintaining overall accuracy in federated learning settings. The general prompt is optimized using a contrastive loss:

$$\mathcal{L}_{ge} = -\frac{1}{N} \sum_{i=1}^N \log \frac{\exp(\cos(\mathbf{t}_g^i, \mathbf{z}_i)/\tau)}{\sum_{j=1}^C \exp(\cos(\mathbf{t}_g^j, \mathbf{z}_j)/\tau)}, \quad (1)$$

where $\mathbf{z}_i = f(\mathbf{x}_i)$ represents the image feature. The text feature $\mathbf{t}_g^i = g([\mathbf{P}_g, \text{CLASS}_i])$ is encoded from the general prompt concatenated with the corresponding class token. Here, C denotes the total number of classes, and τ is the

temperature parameter. However, while the general prompt effectively captures shared features, it may not sufficiently represent the unique characteristics of individual classes, particularly those in the tail of the distribution where samples are scarce and heterogeneous.

Class-Aware Prompt. To address this limitation and the disproportionate effect of prompt tuning on tail classes, we introduce a class-aware prompt $\mathbf{P}_c \in \mathbb{R}^{C \times T \times d}$, where T is the number of learnable tokens per class. This prompt is designed to capture class-specific characteristics, allowing for more nuanced representations of both head and tail classes. For class i , its corresponding prompt is represented as $\mathbf{P}_c^i = [\mathbf{V}_i^1, \mathbf{V}_i^2, \dots, \mathbf{V}_i^T] \in \mathbb{R}^{T \times d}$. During training, only the prompt corresponding to the true class of each sample is updated. The class-aware prompt is optimized using the following loss function:

$$\mathcal{L}_{ca} = -\frac{1}{N} \sum_{i=1}^N \log \frac{\pi_{y_i} \exp(\cos(\mathbf{t}_c^{y_i}, \mathbf{z}_i)/\tau)}{\sum_{j=1}^C \pi_j \exp(\cos(\mathbf{t}_c^j, \mathbf{z}_i)/\tau)}, \quad (2)$$

where y_i is the true class of sample i , $\mathbf{t}_c^j = g([\mathbf{P}_c^j, \text{CLASS}_j])$ is the text feature encoded from the class-aware prompt concatenated with the corresponding class token, and π_j is the global prior probability of class j to handle the long-tailed distribution. Along with the general prompt, the dual-prompt learning mechanism can effectively balance between learning shared domain-invariant representations and class-specific characteristics, thereby enabling robust knowledge transfer across clients while preserving fine-grained features particularly beneficial for tail classes.

Vision-Language Alignment. While our dual-prompt mechanism effectively learns both general and class-specific features in the text domain, there remains a challenge in aligning these textual representations with their

corresponding visual features. To bridge this semantic gap and enhance the interaction between visual and textual modalities, we introduce a vision-language alignment mechanism. Inspired by MaPLe [12], we design a mapping function $\mathcal{F} : \mathbb{R}^d \rightarrow \mathbb{R}^v$ that aligns the learned language prompts with the visual feature space:

$$\mathbf{z}'_i = f([x_i, \tilde{P}_g]), \quad \text{where} \quad \tilde{P}_g = \mathcal{F}(P_g). \quad (3)$$

For each sample, we combine the general and class-aware prompts to form an integrated prompt representation: $P_i = [P_g, P_c^{y_i}, \text{CLASS}_i]$, which is then processed through CLIP’s text encoder: $\mathbf{t}_i = g(P_i)$. To optimize this multi-modal framework, we propose a joint training objective that combines general and class-aware prompt learning:

$$\mathcal{L} = \mathcal{L}_{\text{ge}} + \lambda \mathcal{L}_{\text{ca}}, \quad (4)$$

where λ is a balancing parameter. This joint optimization enables our model to simultaneously learn domain-invariant features through the general prompt and class-specific representations through the class-aware prompt while maintaining effective cross-modal alignment in federated long-tailed scenarios.

3.3. Heterogeneity-Aware Client Clustering

To enable effective prompt aggregation across heterogeneous clients while preserving class-specific characteristics, we introduce a heterogeneity-aware client clustering strategy. This strategy comprises two complementary methods: similarity-based and heterogeneity-based clustering.

Similarity-based Clustering. We introduce a similarity-based clustering method that groups clients with similar class distributions together. This allows for more effective aggregation of class-aware prompts within each cluster, as clients with similar class distributions are more likely to benefit from sharing class-specific information. To measure the similarity between clients’ class distributions, we employ the Jensen-Shannon (JS) divergence. For clients i and j , their JS divergence is calculated as:

$$\text{JS}(\mathbf{d}_i || \mathbf{d}_j) = \frac{1}{2} \text{DKL}(\mathbf{d}_i || \mathbf{d}_M) + \frac{1}{2} \text{DKL}(\mathbf{d}_j || \mathbf{d}_M), \quad (5)$$

where \mathbf{d}_i and \mathbf{d}_j are normalized class distribution vectors for the respective clients, $\mathbf{d}_M = \frac{1}{2}(\mathbf{d}_i + \mathbf{d}_j)$, and DKL is the Kullback-Leibler divergence. We construct a similarity matrix \mathbf{S} and apply the K-means algorithm to form clusters. This clustering strategy enables clients to learn from others with similar data distributions while mitigating the adverse effects of incorporating data from clients with significantly different distributions. In the context of long-tailed data, this approach is particularly beneficial for tail classes, as it allows clients with similar rare class distributions to pool their limited data effectively, thereby improving the learning of tail class features without being overwhelmed by head class data from dissimilar clients.

Heterogeneity-based Clustering. To further address the non-IID challenge and balance the representation of head and tail classes, we introduce a heterogeneity-based clustering method. This approach groups clients with complementary class distributions, allowing clients with head classes to collaborate with those possessing tail classes, leading to a more balanced global model. We calculate the complementarity between clients i and j as:

$$\text{Comp}(\mathbf{d}_i, \mathbf{d}_j) = \sum_{c \in \mathcal{H} \cup \mathcal{T}} \mathbf{d}_i(c)(1 - \mathbf{d}_j(c)), \quad (6)$$

where \mathcal{H} and \mathcal{T} denote the sets of head and tail classes, respectively. Based on this measure, we construct a complementarity matrix \mathbf{C} and apply K-means clustering. The primary objective of this heterogeneity-based clustering is to ensure that each cluster contains a balanced mix of clients with head classes and those with tail classes. Within these heterogeneous clusters, we aggregate the general prompts from all clients. By balancing head and tail class representations within clusters, it mitigates biases towards head classes, addresses non-IID data challenges, and promotes the synthesis of diverse features, ultimately enabling the general prompt to capture more robust and generalized representations across global information.

Communication-Efficient Learning. To optimize communication efficiency while maintaining model performance, we employ an MAB approach to adaptively adjust intra-cluster iterations and global aggregation frequency. This adaptive mechanism helps reduce communication overhead while ensuring effective knowledge sharing across clients. The detailed formulation of the MAB scheduler and parameter updates, and the whole training process algorithm of CAPT are shown in Appendix A.

Remarks: The proposed CAPT framework provides a solution to **RQ 2** through its carefully designed architecture. Through heterogeneity-aware client clustering, the general prompt learns robust universal features by aggregating knowledge from clients with complementary class distributions, effectively handling the non-IID challenge. Meanwhile, the class-aware prompts capture fine-grained discriminative features by grouping clients with similar data patterns, particularly benefiting tail categories where samples are limited and unevenly distributed across clients.

3.4. Privacy discussions of CAPT

It is important to note that the CAPT framework inherently leverages aggregated statistics of client label distributions for clustering. While such aggregated statistical information could potentially pose privacy considerations, we clarify that these distributions are aggregated anonymously and irreversibly, without revealing the raw data or identifiable details from individual clients [9]. Furthermore, the

Table 1. **Performance comparison of CAPT against baseline methods** on long-tailed datasets under different degrees of data heterogeneity (α). Results show accuracy (%) for overall, head, mid, and tail classes. The best results are in **bold**. The second-best results are underlined. Blue numbers indicate improvement of our method over the second-best baseline.

Dataset	Method	$\alpha = 0.05$				$\alpha = 0.1$				$\alpha = 0.5$			
		Overall	Head	Mid	Tail	Overall	Head	Mid	Tail	Overall	Head	Mid	Tail
CIFAR-10-LT	FedCLIP [19]	84.81	98.10	<u>90.20</u>	76.26	85.55	<u>98.45</u>	90.67	77.32	86.26	97.25	89.50	79.92
	PromptFL [6]	88.67	95.30	86.50	<u>84.93</u>	<u>89.32</u>	94.07	88.83	85.23	<u>90.59</u>	96.63	87.43	<u>88.77</u>
	FedTPG [23]	87.78	96.70	87.90	84.14	88.91	96.60	84.70	<u>88.36</u>	88.90	98.30	<u>91.40</u>	83.64
	FedOTP [14]	83.27	83.70	82.13	83.78	85.15	96.65	85.97	80.06	86.97	97.65	86.50	82.98
	FedPGP [4]	<u>88.76</u>	97.05	88.10	84.64	86.96	98.15	84.83	83.76	87.49	<u>97.95</u>	91.23	81.06
	Ours	93.78	<u>97.50</u>	90.47	94.28	93.98	98.60	<u>89.70</u>	94.70	94.04	97.80	93.17	93.06
		$\uparrow 5.02$	$\downarrow 0.60$	$\uparrow 0.27$	$\uparrow 9.35$	$\uparrow 4.66$	$\uparrow 0.15$	$\downarrow 0.97$	$\uparrow 6.34$	$\uparrow 3.45$	$\downarrow 0.50$	$\uparrow 1.77$	$\uparrow 4.29$
CIFAR-100-LT	FedCLIP [19]	61.52	74.83	64.19	49.69	61.46	74.00	63.00	50.83	62.10	74.93	64.16	50.09
	PromptFL [6]	63.21	74.00	<u>68.10</u>	51.60	65.09	<u>76.34</u>	<u>67.16</u>	55.33	65.79	76.03	63.35	60.25
	FedTPG [23]	<u>66.01</u>	67.48	66.84	<u>64.30</u>	64.52	71.17	65.55	58.90	65.56	79.48	<u>69.26</u>	52.60
	FedOTP [14]	60.74	70.45	54.58	57.51	61.22	72.24	61.74	52.62	59.43	75.41	61.68	45.84
	FedPGP [4]	65.07	78.72	64.29	55.77	<u>65.47</u>	76.31	62.77	<u>59.70</u>	<u>66.42</u>	71.17	65.39	<u>63.32</u>
	Ours	72.91	<u>78.59</u>	72.52	69.10	73.89	78.52	73.97	70.47	73.77	<u>79.00</u>	72.52	70.95
		$\uparrow 6.90$	$\downarrow 0.13$	$\uparrow 4.42$	$\uparrow 4.80$	$\uparrow 8.42$	$\uparrow 2.18$	$\uparrow 6.81$	$\uparrow 10.77$	$\uparrow 7.35$	$\downarrow 0.48$	$\uparrow 3.26$	$\uparrow 7.63$
Fashion-MNIST-LT	FedCLIP [19]	73.56	<u>98.70</u>	<u>91.37</u>	52.82	73.66	<u>98.40</u>	<u>91.43</u>	53.10	74.21	97.95	90.37	55.02
	PromptFL [6]	74.21	98.85	88.37	55.86	76.47	98.60	90.50	59.20	77.65	<u>98.80</u>	90.97	61.20
	FedTPG [23]	<u>76.10</u>	96.50	91.00	<u>59.00</u>	<u>77.30</u>	95.50	90.20	<u>62.28</u>	<u>78.24</u>	98.35	<u>91.80</u>	<u>62.06</u>
	FedOTP [14]	73.30	96.25	89.27	54.54	75.65	95.80	86.70	60.96	74.31	99.00	84.97	58.04
	FedPGP [4]	71.31	91.60	87.00	53.78	73.31	98.10	86.60	55.42	77.10	98.95	88.73	61.38
	Ours	83.41	97.15	92.90	72.22	84.63	97.75	93.87	73.84	85.74	98.25	94.47	75.50
		$\uparrow 7.31$	$\downarrow 1.70$	$\uparrow 1.53$	$\uparrow 13.22$	$\uparrow 7.33$	$\downarrow 0.85$	$\uparrow 2.44$	$\uparrow 11.56$	$\uparrow 7.50$	$\downarrow 0.70$	$\uparrow 2.67$	$\uparrow 13.44$

Table 2. **Comparison of CAPT with prompt-tuning methods**. Results show accuracy for overall, head, mid, and tail classes on CIFAR-10-LT, CIFAR-100-LT, and Fashion-MNIST-LT under varying degrees of data heterogeneity. Baseline methods are combined with FedAvg for parameter aggregation. **Bold** indicates best performance, underline indicates second-best performance.

Dataset	Method	$\alpha = 0.05$				$\alpha = 0.1$				$\alpha = 0.5$			
		Overall	Head	Mid	Tail	Overall	Head	Mid	Tail	Overall	Head	Mid	Tail
CIFAR-10-LT	CoCoop+Fedavg	87.77	<u>97.70</u>	90.57	82.12	87.73	95.85	87.97	84.34	88.21	97.05	85.80	86.12
	MaPle+Fedavg	<u>90.39</u>	99.35	89.23	87.50	<u>91.25</u>	98.90	88.40	<u>89.90</u>	<u>92.05</u>	99.20	94.07	87.98
	KgCoOp+Fedavg	88.21	97.05	87.67	85.00	87.67	97.50	85.40	85.10	86.93	<u>97.95</u>	89.20	81.16
	CLIP-LoRA+Fedavg	87.77	89.65	86.10	<u>88.02</u>	87.90	89.31	<u>89.31</u>	88.26	87.91	89.81	86.34	88.09
	Ours	93.78	97.50	<u>90.47</u>	94.28	93.98	<u>98.60</u>	89.70	94.70	94.04	97.80	<u>93.17</u>	93.06
CIFAR-100-LT	CoCoop+Fedavg	59.37	80.14	62.16	42.15	60.85	77.76	64.94	47.35	61.62	77.76	64.94	47.35
	MaPle+Fedavg	<u>70.12</u>	82.17	<u>72.45</u>	59.58	<u>70.50</u>	82.55	74.23	58.88	<u>70.94</u>	85.55	74.45	57.62
	KgCoOp+Fedavg	65.81	79.00	67.48	54.95	66.75	80.83	70.23	53.85	66.99	<u>80.86</u>	71.32	53.58
	CLIP-LoRA+Fedavg	64.97	66.76	65.51	<u>63.25</u>	64.88	66.74	66.74	<u>63.15</u>	64.94	66.59	65.55	<u>63.27</u>
	Ours	72.91	78.59	72.52	69.10	73.89	78.52	<u>73.97</u>	70.47	73.77	79.00	<u>72.52</u>	70.95
Fashion-MNIST-LT	CoCoop+Fedavg	74.23	96.65	90.17	55.70	75.25	<u>99.00</u>	88.67	57.70	77.04	<u>98.70</u>	90.97	60.02
	MaPle+Fedavg	<u>80.56</u>	99.30	93.57	<u>65.26</u>	<u>84.00</u>	99.15	<u>93.37</u>	<u>72.32</u>	84.91	99.20	94.30	<u>73.56</u>
	KgCoOp+Fedavg	73.42	97.05	89.63	54.24	75.15	98.50	88.27	57.94	75.73	98.50	89.20	58.54
	CLIP-LoRA+Fedavg	64.47	90.71	60.29	56.48	64.24	89.99	60.03	56.46	64.51	90.60	61.22	56.05
	Ours	83.41	<u>97.15</u>	<u>92.90</u>	72.22	84.63	97.75	93.87	73.84	85.74	98.25	94.47	75.50

prompt-based learning approach employed in CAPT mitigates privacy leakage risks typically associated with traditional federated learning setups, as gradients from prompts alone significantly limit the effectiveness of gradient inversion attacks [6]. A comprehensive privacy analysis and further discussions are provided in Appendix E.

4. Experiment

4.1. Experimental Setup

Datasets. We evaluate our method on CIFAR-10-LT, CIFAR-100-LT, Fashion-MNIST-LT, and ImageNet-LT

datasets. For the first three datasets, we follow [2] to create long-tailed versions using exponential decay with imbalance factors ($\rho = N_{max}/N_{min}$). For ImageNet-LT, we use the standard version from [18]. Following [35], we analyze performance across Head, Mid, and Tail class groups based on sample frequency.

Baselines. We evaluate CAPT against state-of-the-art methods in both federated learning and prompt-tuning domains using ViT-B/16 as the backbone architecture. We compare with FedCLIP [19] and PromptFL [6], which are representative CLIP-based federated learning methods, as

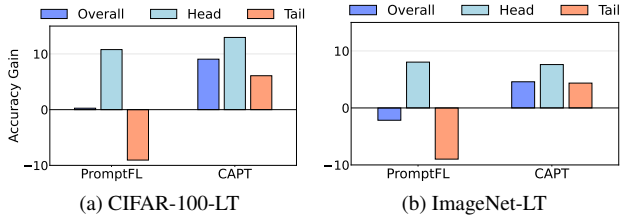


Figure 3. **Accuracy gains (%) comparison between PromptFL and CAPT relative to CLIP.** CAPT achieves superior performance across **head classes**, **tail classes**, and **overall categories**, with particularly significant improvements on **tail classes**

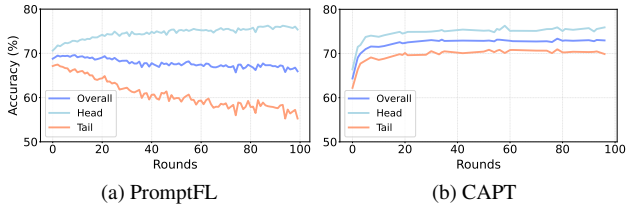


Figure 4. Training dynamics comparison between PromptFL and CAPT on ImageNet-LT dataset.

well as FedTPG [23], FedOTP [14], and FedPGP [4], which focus on personalization in federated prompt learning. We also evaluate against conventional prompt-tuning methods (CoCoop [47], KgCoOp [40], MaPle [12], and CLIP-LoRA [42]) combined with FedAvg [22] for parameter aggregation. Additionally, we conduct experiments with ResNet-50 backbone to compare with traditional federated learning methods trained from scratch, including CReFF [29], FedGrab [36], FedLoge [35], and RUCR [9].

Implementation Details. We implement CAPT using PyTorch and evaluate it on ResNet-50 and ViT-B/16 backbones. In our federated learning setup, we use 20 clients with non-IID data distribution controlled by a Dirichlet parameter α . We perform training for a total of 100 communication rounds using SGD, randomly selecting 40% of the clients to participate in each round. The balancing parameter λ in Eq. (4) is set to 1. For the heterogeneity-aware clustering strategy, we configure the number of clusters K to 3 based on empirical results in Appendix D, which show robust performance across a range of cluster numbers. Further implementation details are provided in Appendix B.

4.2. Comparison with State-of-the-art Methods

Small-scale Datasets Comparison. For small-scale datasets, we compare CAPT with three categories of methods: CLIP-based federated learning approaches, federated versions of centralized CLIP fine-tuning methods, and state-of-the-art federated learning methods specifically designed to address class imbalance.

Tab. 1 compares CAPT with state-of-the-art CLIP-based federated learning methods across various data heterogeneity levels. Results consistently demonstrate CAPT’s supe-

Table 3. Comparison of CAPT with state-of-the-art methods on ImageNet-LT under various non-IID settings.

# α	Method	Overall	Head	Mid	Tail
0.05	FedCLIP [19]	60.51	63.90	58.72	56.47
	PromptFL [6]	65.54	75.22	64.05	56.50
	FedTPG [23]	66.18	70.16	65.27	61.93
	MaPle+FedAvg	65.75	75.88	63.75	54.93
	Ours	73.06	75.71	72.92	70.04
0.1	FedCLIP [19]	60.83	64.25	58.93	56.63
	PromptFL [6]	66.14	75.94	64.59	57.02
	FedTPG [23]	67.06	71.86	65.07	62.82
	MaPle+FedAvg	65.77	76.59	64.33	55.12
	Ours	73.36	75.92	72.61	70.96
0.5	FedCLIP [19]	65.43	70.14	64.69	61.89
	PromptFL [6]	67.87	77.00	65.60	59.76
	FedTPG [23]	68.21	73.41	66.68	63.54
	MaPle+FedAvg	67.61	77.95	65.25	57.93
	Ours	74.01	76.96	73.06	71.19

rior performance in overall accuracy and tail class effectiveness. Fig. 3 further highlights these improvements, showing balanced accuracy gains for CAPT across head-to-tail classes, while PromptFL suffers significant tail-class degradation. More extensive experimental results across different imbalance factors and heterogeneity levels can be found in Appendix C, which further demonstrates CAPT’s consistently superior performance under various settings.

To investigate the efficacy of simply federating state-of-the-art centralized CLIP fine-tuning methods for federated long-tailed learning, we compare CAPT with federated versions of CoCoop [47], MaPle [12], KgCoOp [40], and CLIP-LoRA [42] in Tab. 2. Our results indicate that CAPT consistently outperforms these methods across different datasets and varying heterogeneity levels, underscoring the significance of CAPT’s class-aware prompt design and heterogeneity-aware client clustering in tackling the unique challenges of federated long-tailed learning.

Large-scale Dataset Comparison. For the large-scale ImageNet-LT dataset, we conduct comprehensive evaluations across different heterogeneity levels, with results presented in Tab. 3. The experimental results consistently demonstrate that CAPT effectively learns from scarce and heterogeneous data, maintaining robustness to client heterogeneity. A further analysis of training dynamics, Fig. 4 reveals that CAPT preserves stable and balanced accuracy for both head and tail classes throughout training, while PromptFL experiences a widening performance gap due to declining tail-class accuracy. These findings validate CAPT’s ability to mitigate class imbalance and achieve stable optimization in federated long-tailed scenarios.

Furthermore, CAPT demonstrates superior performance compared to state-of-the-art federated long-tail learning methods using ResNet backbones, achieving consistent improvements in both overall accuracy and balanced performance across all class categories. More detailed compara-

Table 4. Ablation study of CAPT components, comparing different prompt types and cluster aggregation strategies.

Method		CIFAR-10-LT			
		Overall	Head	Mid	Tail
w/o Clu.	General Prompt	89.23	97.50	90.95	84.93
	Class-aware Prompt	90.27	98.75	91.53	86.12
	Gen+Cla	90.42	99.30	91.27	86.36
w/ Clu.	General Prompt	92.00	94.55	90.57	91.84
	Class-aware Prompt	92.69	96.85	90.00	92.64
	Gen+Cla	94.04	97.80	93.17	93.06

Table 5. Ablation study on vision-language alignment and MAB scheduler components across different heterogeneity degrees (α).

V-L	MAB	CIFAR-10-LT			CIFAR-100-LT		
		0.05	0.1	0.5	0.05	0.1	0.5
✓		92.29	93.46	93.22	69.93	70.83	71.70
	✓	92.10	91.97	92.30	68.60	68.12	68.19
✓	✓	93.78	93.98	94.04	72.91	73.89	73.77

tive experiments and analysis on ResNet-based models can be found in Appendix C. These results answer **RQ 3** by demonstrating that CAPT successfully improves tail class performance without sacrificing head class accuracy.

4.3. Ablation Studies

Impact of Prompt Design and Clustering Strategy. We examine the effectiveness of our multi-modal prompt design by comparing general prompt, class-aware prompt, and their combination (Gen+Cla). As shown in Tab. 4, the class-aware prompt outperforms the general prompt across all class categories, demonstrating the importance of capturing class-specific features in long-tailed scenarios. Moreover, the introduction of our heterogeneity-aware client clustering strategy (w/Clu.) significantly boosts performance across all prompt configurations, with particularly notable improvements in tail class performance. Interestingly, we observe that when clustering is applied, the performance gap between different prompt configurations narrows, particularly for tail classes. This suggests that our clustering strategy effectively mitigates the challenges of data heterogeneity, allowing even simpler prompt designs to achieve competitive levels of performance.

To provide insights into the learned representations, we visualize the features extracted by CAPT’s general and class-aware prompts using t-SNE in Fig. 5, where different colors denote different classes in CIFAR-10 and coarse-grained categories in CIFAR-100. The visualization reveals that features learned by the general prompt are more concentrated and generalized, clustering towards the center, indicating the capture of domain-invariant features. In contrast, the class-aware prompt learns more distinctive features, with data points spreading towards the edges, aligning with our design intention of capturing fine-grained, class-

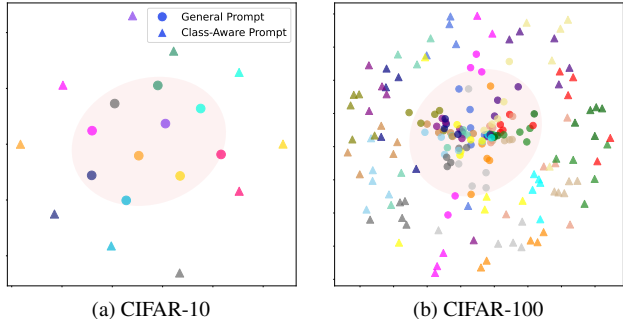


Figure 5. t-SNE visualization of General Prompt (●) and Class-Aware Prompt (▲) embeddings. The shaded area illustrates the region where General Prompt features are clustered.

specific information. This dual representation contributes to CAPT’s strong performance across head, mid, and tail classes in federated long-tailed scenarios.

Impact of Vision-Language Alignment and MAB Scheduler.

We conduct ablation studies on CIFAR-10-LT and CIFAR-100-LT to evaluate our key components. As shown in Tab. 5, the vision-language alignment mechanism consistently improves across all imbalance settings, with larger gains in more imbalanced scenarios. While the MAB scheduler alone shows moderate improvements through its adaptive communication strategy, the combination of both components yields the best results.

Influence of Similarity Metrics and Clustering Parameters.

We investigate the sensitivity of CAPT to different similarity metrics, clustering techniques, and numbers of clusters. Our results indicate that CAPT is robust across various clustering methods and similarity metrics, consistently achieving strong performance with minimal variation. Regarding the number of clusters, our analysis demonstrates stable performance across a moderate range of cluster numbers, underscoring the robustness and practicality of our clustering strategy. More detailed experimental quantitative results and analysis are presented in Appendix D.

5. Conclusion

In this paper, we proposed CAPT, a novel framework for federated learning that effectively addresses long-tailed data distributions and client heterogeneity. Our approach introduces a dual-prompt design with general and class-aware prompts coupled with a heterogeneity-aware client clustering strategy. CAPT significantly improves performance on tail classes while maintaining competitive accuracy on head classes. Notably, CAPT achieves substantial improvements in overall accuracy and tail class performance compared to state-of-the-art methods across various degrees of data heterogeneity. These results highlight CAPT’s effectiveness in tackling the challenges of federated long-tailed learning, paving the way for more robust and equitable machine learning models in decentralized settings.

References

- [1] Adrian Bulat and Georgios Tzimiropoulos. Lasp: Text-to-text optimization for language-aware soft prompting of vision & language models. In *Proceedings of the IEEE/CVF Conference on Computer Vision and Pattern Recognition*, pages 23232–23241, 2023. 3
- [2] Kaidi Cao, Colin Wei, Adrien Gaidon, Nikos Arechiga, and Tengyu Ma. Learning imbalanced datasets with label-distribution-aware margin loss. *Advances in neural information processing systems*, 32, 2019. 6
- [3] Haokun Chen, Ahmed Frikha, Denis Krompass, Jindong Gu, and Volker Tresp. Fraug: Tackling federated learning with non-iid features via representation augmentation. In *Proceedings of the IEEE/CVF International Conference on Computer Vision*, pages 4849–4859, 2023. 1
- [4] Tianyu Cui, Hongxia Li, Jingya Wang, and Ye Shi. Harmonizing generalization and personalization in federated prompt learning. In *Proceedings of the 41st International Conference on Machine Learning*, pages 9646–9661, 2024. 3, 6, 7
- [5] Alexey Dosovitskiy. An image is worth 16x16 words: Transformers for image recognition at scale. *arXiv preprint arXiv:2010.11929*, 2020. 1
- [6] Tao Guo, Song Guo, Junxiao Wang, Xueyang Tang, and Wenchao Xu. Promptfi: Let federated participants cooperatively learn prompts instead of models – federated learning in age of foundation model. *IEEE Transactions on Mobile Computing*, 23(5):5179–5194, 2024. 2, 3, 6, 7, 4, 5
- [7] Kaiming He, Xiangyu Zhang, Shaoqing Ren, and Jian Sun. Deep residual learning for image recognition. In *Proceedings of the IEEE Conference on Computer Vision and Pattern Recognition*, pages 770–778, 2016. 1
- [8] Tony Huang, Jack Chu, and Fangyun Wei. Unsupervised prompt learning for vision-language models. *arXiv preprint arXiv:2204.03649*, 2022. 3
- [9] Wenke Huang, Yuxia Liu, Mang Ye, Jun Chen, and Bo Du. Federated learning with long-tailed data via representation unification and classifier rectification. *IEEE Transactions on Information Forensics and Security*, 2024. 1, 5, 7, 3, 4
- [10] Yangsibo Huang, Samyak Gupta, Zhao Song, Kai Li, and Sanjeev Arora. Evaluating gradient inversion attacks and defenses in federated learning. *Advances in neural information processing systems*, 34:7232–7241, 2021. 4
- [11] Peter Kairouz, H Brendan McMahan, Brendan Avent, Aurélien Bellet, Mehdi Bennis, Arjun Nitin Bhagoji, Kallista Bonawitz, Zachary Charles, Graham Cormode, Rachel Cummings, et al. Advances and open problems in federated learning. *Foundations and Trends® in Machine Learning*, 14(1–2):1–210, 2021. 1
- [12] Muhammad Uzair Khattak, Hanoona Rasheed, Muhammad Maaz, Salman Khan, and Fahad Shahbaz Khan. Maple: Multi-modal prompt learning. In *Proceedings of the IEEE/CVF Conference on Computer Vision and Pattern Recognition*, pages 19113–19122, 2023. 2, 3, 5, 7
- [13] Alex Krizhevsky, Geoffrey Hinton, et al. Learning multiple layers of features from tiny images. 2009. 1
- [14] Hongxia Li, Wei Huang, Jingya Wang, and Ye Shi. Global and local prompts cooperation via optimal transport for federated learning. In *Proceedings of the IEEE/CVF Conference on Computer Vision and Pattern Recognition*, pages 12151–12161, 2024. 3, 6, 7
- [15] Kan Li, Yang Li, Ji Zhang, Xin Liu, and Zhichao Ma. Federated deep long-tailed learning: A survey. *Neurocomputing*, 595:127906, 2024. 1, 2, 3
- [16] Mengke Li, Yiu-ming Cheung, and Yang Lu. Long-tailed visual recognition via gaussian clouded logit adjustment. In *Proceedings of the IEEE/CVF Conference on Computer Vision and Pattern Recognition*, pages 6929–6938, 2022. 1
- [17] Xiaoxiao Li, Meirui Jiang, Xiaofei Zhang, Michael Kamp, and Qi Dou. Fedbn: Federated learning on non-iid features via local batch normalization. In *9th International Conference on Learning Representations, ICLR 2021, Virtual Event, Austria, May 3-7, 2021*, 2021. 1
- [18] Ziwei Liu, Zhongqi Miao, Xiaohang Zhan, Jiayun Wang, Boqing Gong, and Stella X Yu. Large-scale long-tailed recognition in an open world. In *Proceedings of the IEEE/CVF Conference on Computer Vision and Pattern Recognition*, pages 2537–2546, 2019. 6, 1
- [19] Wang Lu, Xixu Hu, Jindong Wang, and Xing Xie. Fedclip: Fast generalization and personalization for CLIP in federated learning. *IEEE Data Engineering Bulletin*, 46(1):52–66, 2023. 2, 6, 7
- [20] Yang Lu, Yiu-Ming Cheung, and Yuan Yan Tang. Bayes imbalance impact index: A measure of class imbalanced data set for classification problem. *IEEE Transactions on Neural Networks and Learning Systems*, 31(9):3525–3539, 2020. 1
- [21] Yang Lu, Pinxin Qian, Gang Huang, and Hanzhi Wang. Personalized federated learning on long-tailed data via adversarial feature augmentation. In *IEEE International Conference on Acoustics, Speech and Signal Processing (ICASSP)*, pages 1–5. IEEE, 2023. 1
- [22] Brendan McMahan, Eider Moore, Daniel Ramage, Seth Hampson, and Blaise Aguera y Arcas. Communication-efficient learning of deep networks from decentralized data. In *Proceedings of the 20th International Conference on Artificial Intelligence and Statistics*, pages 1273–1282. PMLR, 2017. 1, 7, 3
- [23] Chen Qiu, Xingyu Li, Chaithanya Kumar Mummadi, Madan Ravi Ganesh, Zhenzhen Li, Lu Peng, and Wan-Yi Lin. Federated text-driven prompt generation for vision-language models. In *The Twelfth International Conference on Learning Representations*, 2024. 6, 7
- [24] Alec Radford, Jong Wook Kim, Chris Hallacy, Aditya Ramesh, Gabriel Goh, Sandhini Agarwal, Girish Sastry, Amanda Askell, Pamela Mishkin, Jack Clark, et al. Learning transferable visual models from natural language supervision. In *Proceedings of the 38th International Conference on Machine Learning*, pages 8748–8763. PMLR, 2021. 2, 3
- [25] Douglas A Reynolds et al. Gaussian mixture models. *Encyclopedia of biometrics*, 741(659-663), 2009. 3
- [26] Yossi Rubner, Carlo Tomasi, and Leonidas J Guibas. The earth mover’s distance as a metric for image retrieval. *International journal of computer vision*, 40:99–121, 2000. 3

- [27] Dipankar Sarkar, Ankur Narang, and Sumit Rai. Fed-focal loss for imbalanced data classification in federated learning. *arXiv preprint arXiv:2011.06283*, 2020. 2
- [28] Xinyi Shang, Yang Lu, Yiu-ming Cheung, and Hanzi Wang. Fedic: Federated learning on non-iid and long-tailed data via calibrated distillation. In *2022 IEEE International Conference on Multimedia and Expo (ICME)*, pages 1–6. IEEE, 2022. 2
- [29] Xinyi Shang, Yang Lu, Gang Huang, and Hanzi Wang. Federated learning on heterogeneous and long-tailed data via classifier re-training with federated features. In *Proceedings of the Thirty-First International Joint Conference on Artificial Intelligence*, pages 2218–2224, 2022. 1, 2, 7, 3
- [30] Jiangming Shi, Shanshan Zheng, Xiangbo Yin, Yang Lu, Yuan Xie, and Yanyun Qu. Clip-guided federated learning on heterogeneous and long-tailed data. *arXiv preprint arXiv:2312.08648*, 2023. 3
- [31] Ximeng Sun, Ping Hu, and Kate Saenko. Dualcoop: Fast adaptation to multi-label recognition with limited annotations. In *Advances in Neural Information Processing Systems*, 2022. 3
- [32] Grant Van Horn, Oisín Mac Aodha, Yang Song, Yin Cui, Chen Sun, Alex Shepard, Hartwig Adam, Pietro Perona, and Serge Belongie. The inaturalist species classification and detection dataset. In *Proceedings of the IEEE Conference on Computer Vision and Pattern Recognition*, pages 8769–8778, 2018. 3
- [33] Lixu Wang, Shichao Xu, Xiao Wang, and Qi Zhu. Addressing class imbalance in federated learning. In *Proceedings of the AAAI Conference on Artificial Intelligence*, pages 10165–10173, 2021. 2
- [34] Han Xiao, Kashif Rasul, and Roland Vollgraf. Fashion-mnist: a novel image dataset for benchmarking machine learning algorithms. *arXiv preprint arXiv:1708.07747*, 2017. 1
- [35] Zikai Xiao, Zihan Chen, Liyinglan Liu, Yang Feng, Joey Tianyi Zhou, Jian Wu, Wanlu Liu, Howard Hao Yang, and Zuozhu Liu. Fedloge: Joint local and generic federated learning under long-tailed data. In *The Twelfth International Conference on Learning Representations*, 2024. 1, 3, 6, 7
- [36] Zikai Xiao, Zihan Chen, Songshang Liu, Hualiang Wang, Yang Feng, Jin Hao, Joey Tianyi Zhou, Jian Wu, Howard Yang, and Zuozhu Liu. Fed-grab: Federated long-tailed learning with self-adjusting gradient balancer. *Advances in Neural Information Processing Systems*, 36, 2024. 1, 2, 7, 3, 4
- [37] Qiang Yang, Yang Liu, Tianjian Chen, and Yongxin Tong. Federated machine learning: Concept and applications. *ACM Transactions on Intelligent Systems and Technology (TIST)*, 10(2):1–19, 2019. 1
- [38] Wenkai Yang, Deli Chen, Hao Zhou, Fandong Meng, Jie Zhou, and Xu Sun. Integrating local real data with global gradient prototypes for classifier re-balancing in federated long-tailed learning. *arXiv preprint arXiv:2301.10394*, 2023. 2
- [39] Dezhong Yao, Wanning Pan, Yutong Dai, Yao Wan, Xiaofeng Ding, Chen Yu, Hai Jin, Zheng Xu, and Lichao Sun. Fedgkd: Toward heterogeneous federated learning via global knowledge distillation. *IEEE Transactions on Computers*, 73(1):3–17, 2024. 1
- [40] Hantao Yao, Rui Zhang, and Changsheng Xu. Visual-language prompt tuning with knowledge-guided context optimization. In *Proceedings of the IEEE/CVF Conference on Computer Vision and Pattern Recognition*, pages 6757–6767, 2023. 3, 7
- [41] Xin Yao, Tianchi Huang, Chenglei Wu, Ruixiao Zhang, and Lifeng Sun. Towards faster and better federated learning: A feature fusion approach. In *2019 IEEE International Conference on Image Processing (ICIP)*, pages 175–179. IEEE, 2019. 1
- [42] Maxime Zanella and Ismail Ben Ayed. Low-rank few-shot adaptation of vision-language models. In *Proceedings of the IEEE/CVF Conference on Computer Vision and Pattern Recognition*, pages 1593–1603, 2024. 7
- [43] Yaopei Zeng, Lei Liu, Li Liu, Li Shen, Shaoguo Liu, and Baoyuan Wu. Global balanced experts for federated long-tailed learning. In *Proceedings of the IEEE/CVF International Conference on Computer Vision*, pages 4815–4825, 2023. 1, 2
- [44] Renrui Zhang, Xiangfei Hu, Bohao Li, Siyuan Huang, Hanqiu Deng, Yu Qiao, Peng Gao, and Hongsheng Li. Prompt, generate, then cache: Cascade of foundation models makes strong few-shot learners. In *Proceedings of the IEEE/CVF Conference on Computer Vision and Pattern Recognition*, pages 15211–15222, 2023. 2
- [45] Yifan Zhang, Bingyi Kang, Bryan Hooi, Shuicheng Yan, and Jiashi Feng. Deep long-tailed learning: A survey. *IEEE Transactions on Pattern Analysis and Machine Intelligence*, 45(9):10795–10816, 2023. 1
- [46] Yue Zhao, Meng Li, Liangzhen Lai, Naveen Suda, Damon Civin, and Vikas Chandra. Federated learning with non-iid data. *arXiv preprint arXiv:1806.00582*, 2018. 1
- [47] Kaiyang Zhou, Jingkang Yang, Chen Change Loy, and Ziwei Liu. Conditional prompt learning for vision-language models. In *Proceedings of the IEEE/CVF Conference on Computer Vision and Pattern Recognition*, pages 16816–16825, 2022. 3, 7
- [48] Kaiyang Zhou, Jingkang Yang, Chen Change Loy, and Ziwei Liu. Learning to prompt for vision-language models. *International Journal of Computer Vision*, 130(9):2337–2348, 2022. 2, 3
- [49] Ligeng Zhu, Zhijian Liu, and Song Han. Deep leakage from gradients. In *Advances in Neural Information Processing Systems*, 2019. 4

CAPT: Class-Aware Prompt Tuning for Federated Long-Tailed Learning with Vision-Language Model

Supplementary Material

A. Method Details

Training Process. Algorithm 1 outlines the training procedure for our Class-Aware Prompt Tuning (CAPT) method. At each round, selected clients perform local training to update their prompts and coupling function. The server performs clustering-based aggregation on the class-aware and general prompts to enable knowledge sharing across clients.

Algorithm 1: CAPT: Class-Aware Prompt Tuning for Federated Long-tailed Learning

Input: Number of clients K , communication rounds T

Output: General prompt P_g , class-aware prompts P_c , coupling function \mathcal{F}

Initialize P_g, P_c, \mathcal{F} , MAB arms;

for $t = 1$ **to** T **do**

 Randomly select a set of active clients S_t ;

for $k \in S_t$ **do**

 Update $P_g^k, P_c^k, \mathcal{F}^k$ via local training;

end

$\mathcal{C}_s \leftarrow$ Similarity-based clustering;

 Aggregate and distribute $\{P_c^k | k \in c\}$ for each $c \in \mathcal{C}_s$;

$\mathcal{C}_h \leftarrow$ Heterogeneity-based clustering;

 Aggregate and distribute $\{P_g^k | k \in c\}$ for each $c \in \mathcal{C}_h$;

if $MABSelect()$ **then**

 Aggregate and distribute P_g, P_c, \mathcal{F} ;

 UpdateMAB();

end

end

return P_g, P_c, \mathcal{F} ;

Communication-Efficient Learning. To optimize communication efficiency while maintaining model performance, we employ a Multi-Armed Bandit (MAB) approach to adaptively adjust intra-cluster iterations and global aggregation frequency. The MAB scheduler is formulated as follows:

$$V_{k+1}(a) = V_k(a) + \eta_k \cdot (r_k - V_k(a)), \quad (7)$$

where $V_k(a)$ is the estimated value of arm a at round k , r_k is the observed reward, and η_k is a decaying learning

rate. The MAB scheduler selects an arm using an ϵ -greedy strategy with an exploration bonus term:

$$a_k = \arg \max_a \left[\frac{V_k(a)}{N_k(a) + \epsilon} + c \cdot \sqrt{\frac{\log \sum_a N_k(a)}{N_k(a) + \epsilon}} \right]. \quad (8)$$

B. Experimental Details

Datasets. We evaluate our method on four long-tailed datasets: CIFAR-10-LT, CIFAR-100-LT, Fashion-MNIST-LT, and ImageNet-LT. Following [29], we create long-tailed versions of CIFAR-10, CIFAR-100 [13], and Fashion-MNIST [34] by sampling with an exponential decay controlled by the imbalance factor $\rho = N_{max}/N_{min}$, where N_{max} and N_{min} are the number of samples in the most and least frequent classes, respectively. We use imbalance factors of 100, 50, and 10 for CIFAR-10-LT, CIFAR-100-LT, and Fashion-MNIST-LT. For ImageNet-LT, we use the version described in [18], with class sizes ranging from 5 to 1,280 samples. All datasets maintain their original test sets. Following [35], we categorize classes into Head, Mid, and Tail groups by first sorting all classes based on their sample count, then setting two thresholds (75% and 95%) to segregate them. We report accuracy across these three groups to provide a comprehensive evaluation of our method’s performance on varying levels of data scarcity.

Implementation Details. We implemented our proposed method, CAPT, as well as all baselines using PyTorch. We report the performance on two representative and influential backbone architectures, ResNet50 [7] and ViT-B16 [5].

- In the federated learning setting, we simulate a system with 20 clients, where the local datasets are partitioned using a symmetric Dirichlet distribution with a concentration parameter $\alpha \in \{0.05, 0.1, 0.5\}$ to control the degree of non-IID data. Smaller values of α indicate higher data heterogeneity across clients.
- For local training, we use the SGD optimizer with a constant learning rate of $1e-3$. The batch size is set to 32 for CIFAR-10-LT, CIFAR-100-LT, and Fashion-MNIST-LT, and 256 for ImageNet-LT. We perform 100 rounds of communication training, with 1 local epoch per round for CLIP-based methods and 5 local epochs per round in other cases. In each round, 40% of the clients are randomly selected to participate in the training.

For the prompt-tuning baselines (CoCoop, KgCoOp, MaPle, and CLIP-LoRA), we use the same hyperparameters reported in the original papers. The prompt length is

Table 7. Performance comparison of federated long-tail learning methods with all approaches using ResNet backbone.

Methods	CIFAR-10-LT	CIFAR-100-LT	ImageNet-LT
<i>Training from Scratch:</i>			
FedAvg [22]	58.22	30.47	23.85
CReFF [29]	70.31	32.90	25.98
Fed-Grab [36]	70.51	36.53	32.94
FedLoge [35]	70.54	42.72	35.62
RUCR [9]	71.40	35.58	24.02
<i>Finetuning-based:</i>			
PromptFL [6]	62.68	45.77	58.69
Ours	81.28	53.83	64.19

$\alpha = 0.5$, demonstrating that our method is particularly effective in handling challenging scenarios with high client heterogeneity.

As the imbalance factor decreases from 100 to 10, we observe that while the performance gap between head and tail classes naturally narrows for all methods, CAPT maintains its advantage in both overall and tail class performance. This trend is consistent across different datasets and heterogeneity levels, demonstrating the robustness of our class-aware prompt design and heterogeneity-aware clustering strategy. Notably, CAPT’s performance remains stable even under high data heterogeneity, suggesting that our method effectively addresses both class imbalance and non-IID challenges simultaneously.

The improvements are particularly pronounced in more complex datasets like CIFAR-100-LT, where the challenge of learning discriminative features for tail classes is compounded by the larger number of classes. In these scenarios, CAPT’s dual-prompt mechanism proves especially effective at capturing both shared and class-specific features, leading to more balanced performance across all class categories.

Tab. 7 presents a comprehensive comparison of CAPT with state-of-the-art federated learning methods tailored to handle class imbalance using a ResNet backbone. Despite these methods being highly specialized for addressing long-tailed data distributions, CAPT significantly outperforms all baselines. These results highlight CAPT’s ability to effectively learn from imbalanced data distributions in federated settings, surpassing even the most advanced methods designed specifically for this challenge.

D. Additional Ablation Studies

Impact of Similarity Metrics. We investigate the influence of different similarity metrics on CAPT’s performance across both CIFAR-10-LT and CIFAR-100-LT datasets, as shown in Tab. 8. The results demonstrate that CAPT maintains robust performance across various similarity measures. On CIFAR-10-LT, the Wasserstein distance [26] achieves the highest overall accuracy of 93.95%, while JS

Table 8. Impact of Different Similarity Metrics on CAPT Performance

Similarity Metric	CIFAR-10-LT		CIFAR-100-LT	
	Overall	Tail	Overall	Tail
JS Divergence	93.64	94.68	73.77	70.95
KL Divergence	93.29	93.42	74.11	70.72
Wasserstein	93.95	93.56	73.58	69.97
Total Variation	93.48	94.44	73.96	70.80
Cosine	93.55	94.34	73.93	70.20

Table 9. Impact of Different Clustering Techniques on CAPT Performance

Clustering Method	CIFAR-10-LT		CIFAR-100-LT	
	Overall	Tail	Overall	Tail
DBSCAN	93.34	92.10	73.40	68.70
GMM	93.45	92.86	73.34	69.00
Hierarchical	93.35	91.90	73.34	68.28
K-means	93.49	92.92	73.59	68.88
Spectral	93.22	91.96	73.58	68.10

divergence excels in tail class performance. For CIFAR-100-LT, KL divergence leads in overall accuracy is 74.11%, with JS divergence again showing strong tail class performance. Notably, the performance variation across different metrics is minimal, suggesting that CAPT’s effectiveness is not heavily dependent on the choice of similarity measure. This stability can be attributed to our dual-prompt mechanism’s ability to capture both domain-invariant and class-specific features effectively, regardless of the underlying similarity metric.

Analysis of Clustering Techniques. To further validate CAPT’s robustness, we examine the impact of different clustering algorithms on model performance. As presented in Tab. 9, experimental results reveal consistent performance across various clustering methods, with k-means achieving the highest overall accuracy on both datasets (93.49% on CIFAR-10-LT, 73.59% on CIFAR-100-LT). The GMM approach [25] demonstrates particular strength in handling tail classes, achieving 92.86% and 69.00% tail accuracy on CIFAR-10-LT and CIFAR-100-LT, respectively. This comprehensive evaluation demonstrates that CAPT’s heterogeneity-aware strategy maintains its effectiveness across different clustering paradigms, with k-means offering the best balance between computational efficiency and performance.

Impact of Cluster Numbers. To investigate the optimal number of clusters for both similarity-based and

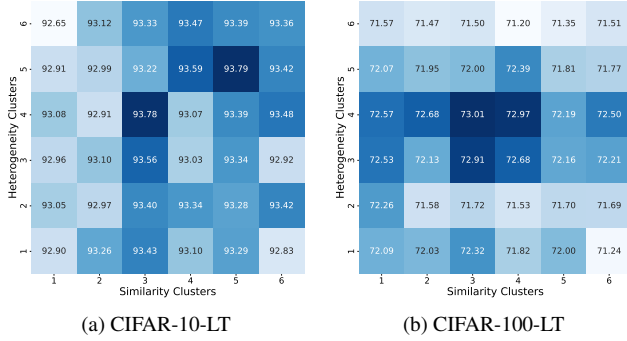


Figure 6. Overall accuracy (%) comparison with different numbers of similarity clusters and dissimilarity clusters on (a) CIFAR-10-LT and (b) CIFAR-100-LT. Darker blue indicates higher accuracy. The results demonstrate that moderate cluster numbers (3-4) generally provide optimal performance across both datasets.

heterogeneity-based clustering strategies, we conduct a comprehensive grid search across different combinations of cluster numbers on CIFAR-10-LT and CIFAR-100-LT datasets. Figure 6 presents the overall accuracy for varying numbers of heterogeneity clusters (y-axis) and similarity clusters (x-axis). On CIFAR-10-LT, we observe that the optimal performance of 93.78% is achieved with 3 similarity clusters and 4 heterogeneity clusters, while CIFAR-100-LT achieves the best accuracy of 73.01% with the same configuration. Our analysis reveals that overly small cluster numbers (1-2) fail to effectively capture the heterogeneity patterns across clients, resulting in suboptimal performance. Conversely, excessive clustering (5-6) leads to fragmentation of limited tail class data without performance benefits. The moderate cluster numbers (3-4) provide the optimal balance between capturing client diversity and maintaining effective knowledge sharing.

D.1. Visualization of Client Clustering

To validate the effectiveness of our proposed clustering strategies, we visualize the class distribution patterns across different clients using heatmaps, as shown in Fig. 7. The similarity-based clustering (Fig. 7a) effectively groups clients with similar class distributions, enabling focused learning within each cluster. In contrast, the heterogeneity-based clustering (Fig. 7b) successfully forms complementary client groups with diverse class coverage, facilitating balanced knowledge sharing across the entire class distribution.

E. Discussion of privacy

Our heterogeneity-aware client clustering strategy utilizes the local label proportions from each client. Although sharing class distributions may potentially disclose aggregated information about clients’ data, this practice is not uncommon in federated learning methods designed for long-tailed

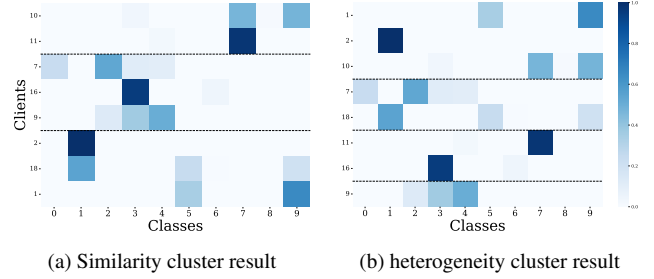


Figure 7. Visualization of client clustering results on CIFAR-10 with non-IID setting ($\alpha = 0.05$). The heatmaps show class distribution patterns where darker colors indicate higher proportions. Dashed lines separate different clusters.

data [9, 36]. These distributions are aggregated in an anonymous and irreversible manner, ensuring that the data distribution of individual clients remains unexposed. Moreover, like all federated learning algorithms, CAPT is susceptible to general privacy risks, such as gradient inversion attacks [49]. However, these risks are not unique to CAPT’s design but are inherent to the federated learning framework [10]. The approach proposed by PromptFL [6] demonstrates that sharing gradients of prompts, rather than full model parameters, can mitigate privacy leakage risks. Specifically, gradient inversion attacks on prompt-based methods fail to reconstruct meaningful data, whereas traditional model-based federated learning is more vulnerable to such attacks. Given that the primary focus of this study is to address the challenges of federated long-tailed learning, an in-depth exploration of privacy mechanisms is beyond the scope of this work, we briefly include the discussion in this subsection.

F. Theoretical Analysis

In this section, we present a rigorous theoretical analysis to demonstrate why traditional prompt tuning methods face challenges in FL with non-IID and long-tailed data. Specifically, we show that such data exacerbates gradient variance, leading to decreased accuracy and hindered convergence.

F.1. Problem Formulation

We consider a federated learning system with K clients and a central server. Each client $k \in \{1, 2, \dots, K\}$ possesses a local dataset $D_k = \{(\mathbf{x}_i^k, y_i^k)\}_{i=1}^{n_k}$ drawn from a local data distribution \mathcal{D}_k , where $\mathbf{x}_i^k \in \mathbb{R}^d$ is an input sample, $y_i^k \in \{1, 2, \dots, C\}$ is the corresponding label, and $n_k = |D_k|$ is the number of samples on client k . The global dataset is $D = \bigcup_{k=1}^K D_k$.

Definition 1 (Imbalance Ratio). *The imbalance ratio ρ is defined as the ratio between the maximum and minimum*

class sample sizes across all clients:

$$\rho = \frac{\max_c \{n_c\}}{\min_c \{n_c\}}, \quad (9)$$

where $n_c = \sum_{k=1}^K n_c^k$ is the total number of samples for class c , and n_c^k is the number of samples of class c on client k .

Definition 2 (Long-Tailed Distribution). *A dataset exhibits a long-tailed distribution if the class sample sizes $\{n_c\}_{c=1}^C$ follow an exponential decay:*

$$n_c = n_{\max} e^{-\alpha c}, \quad (10)$$

where n_{\max} is the maximum class sample size, $\alpha > 0$ is the decay rate, and classes are ordered such that $n_1 \geq n_2 \geq \dots \geq n_C$.

Following PromptFL[6], we make the standard assumptions:

Assumption 1 (Smoothness). *The loss function $\ell(\mathbf{x}, y; \mathbf{P}_s)$ is L -smooth with respect to \mathbf{P}_s :*

$$\|\nabla \ell(\mathbf{x}, y; \mathbf{P}_s) - \nabla \ell(\mathbf{x}, y; \mathbf{P}'_s)\| \leq L \|\mathbf{P}_s - \mathbf{P}'_s\|.$$

Assumption 2 (Bounded Local Variance). *The variance of stochastic gradients on each client is bounded:*

$$\mathbb{E}_{(\mathbf{x}, y) \sim \mathcal{D}_k} [\|\nabla \ell(\mathbf{x}, y; \mathbf{P}_s) - \nabla F_k(\mathbf{P}_s)\|^2] \leq \sigma_k^2,$$

where $\nabla F_k(\mathbf{P}_s) = \mathbb{E}_{(\mathbf{x}, y) \sim \mathcal{D}_k} [\nabla \ell(\mathbf{x}, y; \mathbf{P}_s)]$ is the local gradient on client k .

Assumption 3 (Gradient Diversity). *The gradient dissimilarity among clients is quantified by:*

$$\delta_s^2 = \frac{1}{K} \sum_{k=1}^K \|\nabla F_k(\mathbf{P}_s) - \nabla F(\mathbf{P}_s)\|^2,$$

where $\nabla F(\mathbf{P}_s) = \frac{1}{K} \sum_{k=1}^K \nabla F_k(\mathbf{P}_s)$ is the global gradient.

F.2. Lemmas and Proofs

Lemma 1 (Gradient Variance Decomposition). *The variance of the global gradient estimator can be decomposed into the sum of the within-client variance and the between-client variance:*

$$\begin{aligned} & \mathbb{E} \left[|\nabla \ell(\mathbf{x}, y; \mathbf{P}_s) - \nabla F(\mathbf{P}_s)|^2 \right] \\ &= \frac{1}{K} \sum_{k=1}^K \left(\sigma_k^2 + \|\nabla F_k(\mathbf{P}_s) - \nabla F(\mathbf{P}_s)\|^2 \right). \end{aligned}$$

Proof. By the law of total variance, for any random variable X :

$$\text{Var}(X) = \mathbb{E} [\text{Var}(X|Y)] + \text{Var}(\mathbb{E}[X|Y]).$$

Applying this to the stochastic gradient $\nabla \ell(\mathbf{x}, y; \mathbf{P}_s)$, we have:

$$\begin{aligned} & \mathbb{E} \left[\|\nabla \ell(\mathbf{x}, y; \mathbf{P}_s) - \nabla F(\mathbf{P}_s)\|^2 \right] \\ &= \frac{1}{K} \sum_{k=1}^K \mathbb{E}_{(\mathbf{x}, y) \sim \mathcal{D}_k} \left[\|\nabla \ell(\mathbf{x}, y; \mathbf{P}_s) - \nabla F(\mathbf{P}_s)\|^2 \right] \\ &= \frac{1}{K} \sum_{k=1}^K \left(\mathbb{E}_{(\mathbf{x}, y) \sim \mathcal{D}_k} \left[\|\nabla \ell(\mathbf{x}, y; \mathbf{P}_s) - \nabla F_k(\mathbf{P}_s)\|^2 \right] \right. \\ & \quad \left. + \|\nabla F_k(\mathbf{P}_s) - \nabla F(\mathbf{P}_s)\|^2 \right) \\ &= \frac{1}{K} \sum_{k=1}^K \left(\sigma_k^2 + \|\nabla F_k(\mathbf{P}_s) - \nabla F(\mathbf{P}_s)\|^2 \right). \end{aligned}$$

In the second equality, we used the fact that:

$$\mathbb{E}_{(\mathbf{x}, y) \sim \mathcal{D}_k} [\nabla \ell(\mathbf{x}, y; \mathbf{P}_s)] = \nabla F_k(\mathbf{P}_s).$$

Moreover, the cross term vanishes because:

$$\mathbb{E}_{(\mathbf{x}, y) \sim \mathcal{D}_k} [\nabla \ell(\mathbf{x}, y; \mathbf{P}_s) - \nabla F_k(\mathbf{P}_s)] = 0. \quad \square$$

Lemma 2 (Impact of Class Imbalance on Gradient Discrepancy). *In federated learning with non-IID long-tailed data and imbalance ratio ρ , the squared norm of the gradient discrepancy between client k and the global model is bounded by:*

$$\|\nabla F_k(\mathbf{P}_s) - \nabla F(\mathbf{P}_s)\|^2 \leq G^2 \sum_{c=1}^C (\pi_c^k - \pi_c)^2,$$

where π_c^k and π_c are the class proportions on client k and globally, respectively, and G is an upper bound on the norm of class-specific gradients.

Proof. We express the local and global gradients in terms of class proportions:

$$\begin{aligned} \nabla F_k(\mathbf{P}_s) &= \sum_{c=1}^C \pi_c^k \nabla F_c(\mathbf{P}_s), \\ \nabla F(\mathbf{P}_s) &= \sum_{c=1}^C \pi_c \nabla F_c(\mathbf{P}_s), \end{aligned}$$

where:

- $\pi_c^k = \frac{n_c^k}{n_k}$ is the proportion of class c on client k .
- $\pi_c = \frac{n_c}{n}$ is the global proportion of class c .

- $\nabla F_c(\mathbf{P}_s) = \mathbb{E}_{(\mathbf{x}, y) \sim \mathcal{D}_c} [\nabla \ell(\mathbf{x}, y; \mathbf{P}_s)]$ is the gradient with respect to class c .

Then, the gradient discrepancy taking the squared norm:

$$\begin{aligned} \|\nabla F_k(\mathbf{P}_s) - \nabla F(\mathbf{P}_s)\|^2 &= \left\| \sum_{c=1}^C (\pi_c^k - \pi_c) \nabla F_c(\mathbf{P}_s) \right\|^2 \\ &\leq \left(\sum_{c=1}^C |\pi_c^k - \pi_c| \|\nabla F_c(\mathbf{P}_s)\| \right)^2. \end{aligned}$$

Assuming that the class-specific gradients are bounded, i.e., $\|\nabla F_c(\mathbf{P}_s)\| \leq G$, we have:

$$\|\nabla F_k(\mathbf{P}_s) - \nabla F(\mathbf{P}_s)\|^2 \leq G^2 \left(\sum_{c=1}^C |\pi_c^k - \pi_c| \right)^2.$$

Using the inequality $(\sum_{i=1}^n a_i)^2 \leq n \sum_{i=1}^n a_i^2$, we get:

$$\left(\sum_{c=1}^C |\pi_c^k - \pi_c| \right)^2 \leq C \sum_{c=1}^C (\pi_c^k - \pi_c)^2.$$

Therefore,

$$\|\nabla F_k(\mathbf{P}_s) - \nabla F(\mathbf{P}_s)\|^2 \leq G^2 C \sum_{c=1}^C (\pi_c^k - \pi_c)^2.$$

Alternatively, by ignoring cross terms (assuming gradients are uncorrelated), we can directly write:

$$\|\nabla F_k(\mathbf{P}_s) - \nabla F(\mathbf{P}_s)\|^2 \leq G^2 \sum_{c=1}^C (\pi_c^k - \pi_c)^2.$$

□

Theorem 1 (Convergence Difficulty in Traditional Prompt Tuning). *In federated learning with non-IID long-tailed data exhibiting an imbalance ratio ρ , the gradient variance in traditional prompt tuning methods increases with ρ , leading to slower convergence rates and decreased accuracy. Specifically, the convergence rate is adversely affected by the term:*

$$\delta_s^2 = \frac{1}{K} \sum_{k=1}^K \|\nabla F_k(\mathbf{P}_s) - \nabla F(\mathbf{P}_s)\|^2 \leq G^2 \Delta_\pi^2,$$

where

$$\Delta_\pi^2 = \frac{1}{K} \sum_{k=1}^K \sum_{c=1}^C (\pi_c^k - \pi_c)^2,$$

which increases with the imbalance ratio ρ .

Proof. From Lemma 1, the variance of the global gradient estimator is:

$$\begin{aligned} &\mathbb{E} \left[\|\nabla \ell(\mathbf{x}, y; \mathbf{P}_s) - \nabla F(\mathbf{P}_s)\|^2 \right] \\ &= \frac{1}{K} \sum_{k=1}^K \left(\sigma_k^2 + \|\nabla F_k(\mathbf{P}_s) - \nabla F(\mathbf{P}_s)\|^2 \right). \end{aligned}$$

The term $\delta_s^2 = \frac{1}{K} \sum_{k=1}^K \|\nabla F_k(\mathbf{P}_s) - \nabla F(\mathbf{P}_s)\|^2$ represents the between-client variance, which is affected by data heterogeneity. Using Lemma 2, we have:

$$\delta_s^2 = \frac{1}{K} \sum_{k=1}^K \|\nabla F_k(\mathbf{P}_s) - \nabla F(\mathbf{P}_s)\|^2 \leq G^2 \Delta_\pi^2.$$

□

Lemma 3 (Distribution Discrepancy Under Long-Tailed Setting). *In a non-IID long-tailed setting, the distribution discrepancy measure Δ_π^2 can be expressed in terms of the class-wise variances:*

$$\mathbb{E}_k[\Delta_\pi^2] = \frac{1}{K} \sum_{k=1}^K \sum_{c=1}^C \mathbb{E}_k[(\pi_c^k - \pi_c)^2] = \sum_{c=1}^C \sigma_c^2,$$

where σ_c^2 is the variance of the deviation in class proportions across clients.

Proof. For each class c , we model the client-specific proportion as:

$$\pi_c^k = \pi_c + \epsilon_c^k,$$

where ϵ_c^k represents the deviation from the global proportion with:

$$\begin{aligned} \mathbb{E}_k[\epsilon_c^k] &= 0, \\ \text{Var}_k(\epsilon_c^k) &= \sigma_c^2. \end{aligned}$$

The distribution discrepancy can then be written as:

$$\begin{aligned} \mathbb{E}_k[\Delta_\pi^2] &= \frac{1}{K} \sum_{k=1}^K \sum_{c=1}^C \mathbb{E}_k[(\pi_c^k - \pi_c)^2] \\ &= \frac{1}{K} \sum_{k=1}^K \sum_{c=1}^C \mathbb{E}_k[(\epsilon_c^k)^2] \\ &= \sum_{c=1}^C \sigma_c^2. \end{aligned}$$

□

Lemma 4 (Variance-Proportion Relationship). *The class-wise variance σ_c^2 is proportional to $\pi_c(1 - \pi_c)$, and increases for rare classes as the imbalance ratio ρ grows:*

$$\sigma_c^2 = \beta \pi_c(1 - \pi_c) \cdot g(\rho),$$

where $g(\rho)$ is an increasing function of ρ and $\beta > 0$ is a constant.

Proof. In the long-tailed setting, the class proportions follow an exponential decay:

$$\pi_c = \frac{e^{-\alpha c}}{S} = e^{-\alpha(c-1)}(1 - e^{-\alpha}),$$

where S is the normalizing constant and $\alpha = \frac{\ln(\rho)}{C-1}$. The variance σ_c^2 captures the heterogeneity of class distributions across clients. For rare classes with large c , π_c becomes exponentially smaller as ρ increases, leading to larger relative fluctuations in π_c^k . This relationship is naturally modeled by the binomial variance term $\pi_c(1 - \pi_c)$ scaled by a heterogeneity factor $g(\rho)$ that increases with the imbalance ratio. \square

Theorem 2 (Impact of Imbalance Ratio on Distribution Discrepancy). *The distribution discrepancy measure Δ_π^2 satisfies:*

$$\Delta_\pi^2 = \Theta(h(\rho)),$$

where $h(\rho)$ is a monotonically increasing function with $h(\rho) = \Omega(\log \rho)$.

Proof. From Lemma 3 and Lemma 4, we have:

$$\begin{aligned} \Delta_\pi^2 &= \sum_{c=1}^C \sigma_c^2 = \beta g(\rho) \sum_{c=1}^C \pi_c(1 - \pi_c) \\ &= \beta g(\rho) \sum_{c=1}^C e^{-\alpha(c-1)}(1 - e^{-\alpha})(1 - e^{-\alpha(c-1)}(1 - e^{-\alpha})). \end{aligned}$$

Since $\alpha = \frac{\ln(\rho)}{C-1}$, both the exponential decay of π_c and the heterogeneity factor $g(\rho)$ contribute to the growth of Δ_π^2 . The sum can be bounded below by $\Omega(\log \rho)$, while $g(\rho)$ captures additional heterogeneity effects, yielding the stated asymptotic behavior. \square

Corollary 1 (Impact on Convergence Rate). *The convergence rate of stochastic optimization in non-IID long-tailed settings satisfies:*

$$\frac{1}{T} \sum_{t=1}^T \mathbb{E}[\|\nabla F(\mathbf{P}_s^t)\|^2] \leq \frac{2(F(\mathbf{P}_s^0) - F^*)}{\eta T} + \eta(\sigma^2 + G^2 h(\rho)),$$

with $h(\rho) = \Omega(\log \rho)$, indicating that the convergence rate degrades at least logarithmically with the imbalance ratio.

Proof. Combining Theorem 1 and Theorem 2, we have $\delta_s^2 \leq G^2 \Delta_\pi^2 = G^2 \Theta(h(\rho))$. Substituting into the convergence bound yields:

$$\frac{1}{T} \sum_{t=1}^T \mathbb{E}[\|\nabla F(\mathbf{P}_s^t)\|^2] \leq \frac{2(F(\mathbf{P}_s^0) - F^*)}{\eta T} + \eta(\sigma^2 + G^2 h(\rho)).$$

\square

The presence of the term $\eta G^2 h(\rho)$ indicates that the convergence rate deteriorates as the imbalance ratio increases, with the degradation being amplified by both the learning rate η and the gradient bound G^2 .

Remarks: The theorem indicates that as the imbalance ratio ρ increases, the class proportion differences $(\pi_c^k - \pi_c)$ become larger due to the non-IID and long-tailed nature of the data. This exacerbates the gradient variance across clients, leading to hindered convergence in traditional prompt tuning methods.

This theoretical analysis directly answers **RQ1** by revealing the underlying mechanism of why prompt tuning disproportionately affects tail classes in federated long-tailed scenarios. Specifically, we have shown that: (1) The gradient variance is amplified by the combined effect of non-IID data distribution and long-tailed class imbalance, as evidenced by the term δ_s^2 which increases with the imbalance ratio ρ ; (2) This increased variance particularly impacts tail classes due to their limited samples being further fragmented across heterogeneous clients; and (3) The traditional prompt tuning methods lack mechanisms to compensate for this amplified variance, resulting in degraded performance on tail classes.